

Towards microcrystalline silicon n-i-p solar cells with 10% conversion efficiency

L. Feitknecht, C. Droz, J. Bailat, X. Niquille, J. Guillet, A. Shah

Institut de Microtechnique, Université de Neuchâtel,
Breguet 2, CH-2000 Neuchâtel, Switzerland.

ABSTRACT

High-performance microcrystalline and amorphous silicon solar cells are the key elements for a successful combination to form the "micromorph" tandem cell [1,2]. A microcrystalline silicon ($\mu\text{c-Si:H}$) solar cell in the n-i-p configuration was fabricated by the VHF PE-CVD deposition process. The cell has a conversion efficiency exceeding 9% ($V_{\text{OC}}=520$ mV, $\text{FF}=73\%$, $J_{\text{SC}}=24.2$ mA/cm²). This result was achieved by a successful combination of the following elements: first a fine-tuning of the silane concentration (SC) in hydrogen feedstock gas used for deposition of the intrinsic <i> absorber layer, second, the incorporation of an optimised back-reflecting substrate into the cell; and, third, the ideal combination of each of these key-components.

Compared to earlier results with n-i-p-type $\mu\text{c-Si:H}$ solar cells, a substantial increase in V_{OC} was now obtained, while maintaining reasonable J_{SC} -values. Earlier investigations on the role of the i-layer material had revealed a trade-off between cells with high J_{SC} but low V_{OC} or cells of low J_{SC} and high V_{OC} . In the present contribution the authors now show the successful combination of a cell with an acceptable V_{OC} and good J_{SC} generation in the long-wavelength region (above 700 nm). This is mainly because of suitable light-diffusing back-reflectors which perform well with respect to both, optical and electrical aspects.

INTRODUCTION

The fabrication of substrate-nip solar cells is substantially different from that of superstrate-pin solar cells, because of the change in the deposition sequence of the layers and its technological consequences (like initial n-type or p-type nucleation layer and optically transparent and doped window-layers). Whereas a relatively large number of papers have dealt with the design and fabrication of superstrate-pin cells, only a relatively small number of papers have looked at substrate-nip cells. The present work is a further contribution to latter topic and will deal with a specific problem in this context:

The interface of the back-TCO (transparent conductive oxide) to the n-type silicon film (we call it here the 'back-interface') takes on a very important role for the deposition of nip-type cells and this interface has an influence on the structure of the whole cell and its performance: Indeed, nucleation of silicon grains, electronic and optical properties are key issues which depend on the nature of the underlying back-TCO material [3,4].

Investigations on the interface of the back-TCO / n-layer of the n-i-p solar cell are not straight-forward since the interesting part is hidden by the solar cell and thus not directly accessible. Since most of the light is absorbed within the first 2 μm of the absorber, only the long wavelength part of the light spectrum reaches the back-interface under white-light illumination. A better cell characterisation is possible if the External quantum Efficiency (EQE) measurement is performed from both sides of the cell (double-sided illumination).

EXPERIMENTAL

$\mu\text{c-Si:H}$ silicon n-i-p solar cells were deposited in a single-chamber VHF-GD reactor at plasma excitation frequencies between 70 to 130 MHz. Typical deposition parameters for the intrinsic layer are: base pressure of the vacuum chamber $p_{\text{base}} < 4.1\text{E-}8$ mbar, deposition pressure $p = 0.1\text{-}0.9$ mbar, applied plasma power $P = 5\text{-}30$ W, substrate temperature around 200°C . A gas purifier was used to avoid incorporation of detrimental oxygen contamination [5]. These conditions lead to deposition rates in the region of 3 to 10 \AA/sec .

Stainless steel and glass substrates were prepared for the back-reflectors which consist of a stack of sputtered silver (Ag) and zinc oxide (ZnO); silver is deposited at substrate temperatures around 400°C in order to increase the growth-induced surface-texture (RMS around 60nm). Current vs. voltage characterisation was performed under AM1.5 conditions at 100 mW/cm^2 , using a two-source solar simulator. The short circuit current densities (J_{sc}) were calibrated by the scalar product of the External Quantum Efficiency (EQE) data with the AM1.5 sun spectrum within the range of 350 to 1000 nm. For a better characterisation, we swapped the solar cell in order to illuminate the cell not from the p-side (the normal configuration for thin-film silicon solar cells) but to illuminate the rear-side of the cell i.e. through the glass substrate, the back-TCO and the n-layer. Under the n-side illumination, more information on the behaviour of the junction near the back-interface can be obtained.

RESULTS AND DISCUSSION

Interfaces

We deposited in the same deposition-run a nip-type $\mu\text{c-Si:H}$ cell on substrates which were coated with four different back-TCOs: a) a raw stainless steel plate without any TCO material, b) sputtered ZnO, c) CVD-ZnO and d) CVD-ZnO covered with sputtered ZnO on top; see Figure 1.

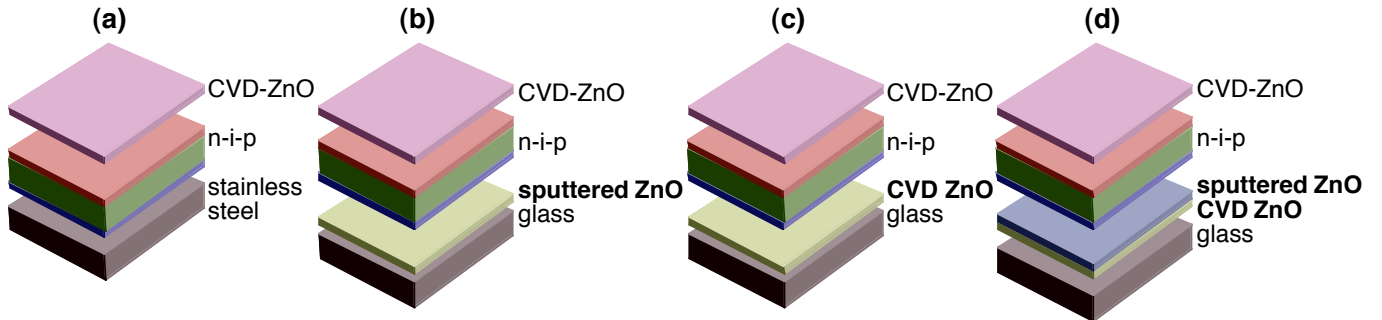


Figure 1: Investigations on the role of the back-interface material: in a single deposition-run, the substrates of (a) stainless steel, (b) glass/sputtered ZnO, (c) glass/CVD-ZnO and (d) glass/CVD-ZnO covered with sputtered ZnO were processed together.

In Table 1, the electronic cell-characteristics given there highlight the relation of the back-interface to the n-type film of the n-i-p cell. There is a close link between the type of TCO material used and the performance of the solar cell. The best conversion efficiency was achieved on the reference substrate without any ZnO, the next best cell is fabricated on the combined ZnO-back contact (a textured CVD ZnO covered with the non-intentionally textured sputtered ZnO). The worst conversion efficiency of this n-i-p cell is reported for the CVD-ZnO back-interface. The EQE curves of these respective cells are given in Figure 2.

Table 1: Electrical performance of the n-i-p solar cells deposited onto four different back-interface configurations:

#	Back-interface	V _{OC} [mV]	FF [%]	V _{OC} .FF [a.u.]	J _{SC} : n/p [mA/cm ²]	ratio [n/p]	□ [%]
a)	Stainless steel	450	71.6	322	n.a. / 20.9	n.a.	6.7
b)	Sputtered ZnO	460	69.0	317	10.9 / 17.1	0.64	5.4
c)	CVD-ZnO	438	64.2	281	5.7 / 17.6	0.32	4.9
d)	CVD + Sputtered ZnO	454	68.3	310	11.9 / 18.7	0.64	5.8

Double-sided quantum efficiency measurement

For interpretation, the external quantum efficiency (EQE) data may be subdivided in three intervals, a first range up to 520 nm, the second from 600 nm to 800 nm and the third from 800 nm to 1000 nm. The EQE illuminated from the n-side is zero up to a wavelength of 520 nm on the back-contact with CVD-ZnO. On the two sputtered samples a considerably higher signal is measured and no difference between the two ZnO types is apparent, but the values obtained by the n-side EQE curve still remains below the values obtained for the p-side illuminated EQE curve of the cell. In the last interval only, the EQE curve of the cell with CVD-ZnO gains over the EQE curve of the cell with a sputtered ZnO back-contact: this is an effect of the good light scattering behaviour of the textured, rough CVD-ZnO.

In all curves of p-side illuminated EQE data, there is a slight dip in the region of 600 nm to 800 nm: this dip is a sign for the absence of a powerful light-trapping scheme, as one would obtain by e.g. optimised back-reflectors. The dip could also be avoided by increased cell absorber thickness (exceeding 2.5 μm).

TEM investigations

The Transversal Electron Microscope (TEM) allows for a close look on the nucleation of microcrystalline films on CVD and sputtered ZnO, see Figure. 3. Crystallographic observations help here to highlight one facet of the situation at the n-i interface.

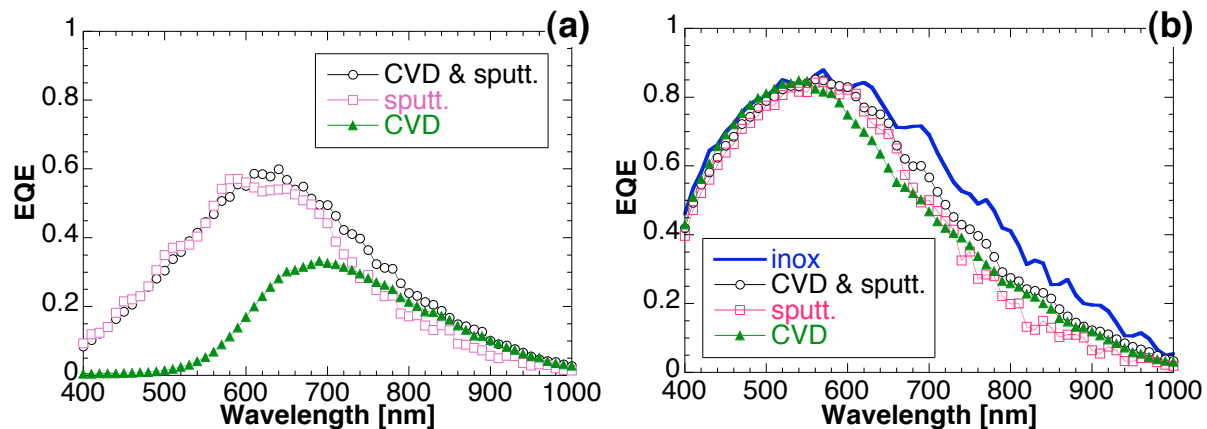


Figure 2: (a) Quantum efficiency measurement illuminated from the n-side and (b) illuminated from the p-side: stainless steel (inox), CVD-ZnO covered with sputtered ZnO, simply sputtered ZnO and CVD-ZnO on glass substrates were utilised respectively.

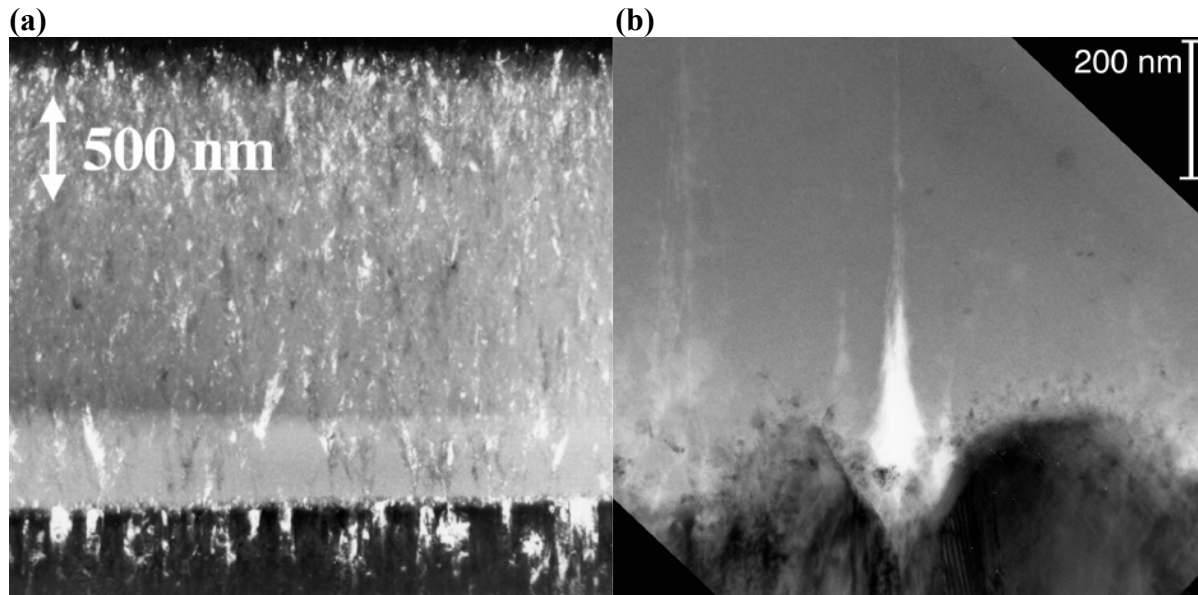


Figure 3: (a) TEM dark field micrograph of a microcrystalline n-i-p solar cell deposited on sputtered ZnO. ZnO is at the bottom of the picture, n-type μ c-Si:H layer appears as a thin dotted layer. (b) TEM bright-field micrograph of the ZnO-n-i interface of a solar cell deposited on CVD ZnO. ZnO tetrahedrons are at the bottom of the picture. Note the disordered grainy contrast of the n-layer. A crack/void at the bottom of the ZnO valley appears bright; source: [4]

Measurements on another series of cells, namely on a “dilution series” of nip-type solar cells (i.e. n-i-p solar cells where the intrinsic <i> i </i> absorber layers were deposited at various silane concentrations) reveal a systematically denser crystalline structure of the n-layer on sputtered ZnO than on CVD ZnO. As a consequence of this different n-layer growth, in the initial stage of i-layer deposition, the beginning of the i-layer consists of a mixed-phase layer (amorphous and microcrystalline parts). This layer (also referred to as 'incubation layer') is reported to vary from 140 nm for cells on sputtered ZnO to 200 nm for cells on CVD-ZnO [4,6].

The back-TCO and the electrical characteristics are correlated: The observations of low EQE curves of cells on CVD-ZnO goes in parallel with a poorly formed n-film as visible in the TEM images. In the following section, we present possible explanations for this.

Discussion on cell interfaces

The difficulty to match a certain nip-type solar cell onto different back-contact materials is discussed in the precedent section. A cell might work well in one specific configuration (i.e. for a specific combination of substrate and cell) and the same cell may then show a considerable drop in performance if just the back-contact material is changed. The thin-film solar cell should not be considered as a combination of correctly optimised independent layers, but as a device of both layers and interfaces which have to be optimised on the device itself. Keeping in mind that not only the physical (e.g. crystallographic) but also chemical (out diffusion) and electronic (transport) aspects play important roles in this question, we draw attention to several possible explanations for the observed incompatibility between our present n-i-p cells and certain, specific back-contacts (e.g. CVD-ZnO, here):

^{1st} If we consider that light of increasing wavelength is absorbed increasingly deeper inside the silicon film, a zone comprising the n-layer and the beginning of the i-layer can be

made responsible for the non-existent carrier generation/collection in the spectral range of 400 to 520 nm, for the case of cells deposited on CVD-ZnO, as seen in Figure 2(a). This might be due to an optical problem (no photon absorption) or to an electronic problem (no electrical field, and thus no carrier separation). The junction would then lack an electrical field within something like 100 nm of the n-i interface. The most plausible explanation for poor n-film quality in these first 100 nm would be difference in surface roughness of these two ZnO types (rough CVD-ZnO and flat sputtered ZnO), since deposition onto a flat surface does not lead to the same layer microstructure, as growth on a textured surface [7]: All of the four investigated back-ZnO contacts have different surface roughness, starting from the flat sputtered ZnO (only 4 nm of rms roughness) up to the very rough CVD-ZnO (60 nm of rms roughness). Note that the surface roughness plays a decisive role in the nucleation of the silicon film. A poor nucleation of the silicon layer closest to the back-interface might cause a poor cell performance.

2nd, cross-contamination due to the first stage of the i-layer growth might cause a poor junction within the region of the back-interface (i.e. the region within the n-type and the i-type \square c-Si:H film). On the other hand, a phosphorus contamination due to the preceding deposition of the n-film can be excluded: The common problem of contamination in cells fabricated in a single-chamber deposition system would disturb the whole batch of cells. In our case here, cells of the same batch but deposited on CVD-ZnO show a poor EQE signal whereas cells deposited on sputtered ZnO back-contacts have a higher EQE signal, if we consider wavelengths below 520 nm. Since absorber layer contamination by a preceding n-film would harm the whole batch of cells, independently of the back-contact material, this type of contamination can indeed be excluded.

3rd The difference of the junction deposited onto the CVD-ZnO and deposited onto the sputtered aluminium doped ZnO layer might be due to an incompatibility of our n-type film with the CVD-ZnO combining physical (e.g. surface roughness) and chemical reasons.

4th Another explanation may be the ZnO surface states which may interact with the deposition plasma of the growing n-type film. Thereby, particles of zinc, oxygen, silicon and phosphorus might get mixed together in the plasma process and create an n-film of a less favourable quality in the case of the CVD-ZnO - something which apparently does not happen on the sputtered ZnO. The term of 'quality' refers here exclusively to crystallographic observations made by TEM, as no doping profile was analysed.

Up to now, not enough measured evidence for or against any of these hypothesis could be given (e.g. SIMS data were not satisfactorily clear). In our eyes, an optimisation of the n-i-p cell interface to the CVD-ZnO back-contact seems generally possible but was so far beyond the reach of this study.

CONCLUSIONS

The importance of 'interface-tailoring' for n-i-p solar cells has been made evident in this paper, by giving results on the investigation of four different back-contacts. One must always remember that a thin-film solar cell is not simply a stack of layers but a complex device resulting from an optimal fit of interacting layers. Special care is needed here at the "back-contact interface", i.e. at the interface substrate-silicon. The measurement of quantum efficiency illuminated from both sides contributed considerably to the detection of malfunctions of this "back-contact interface".

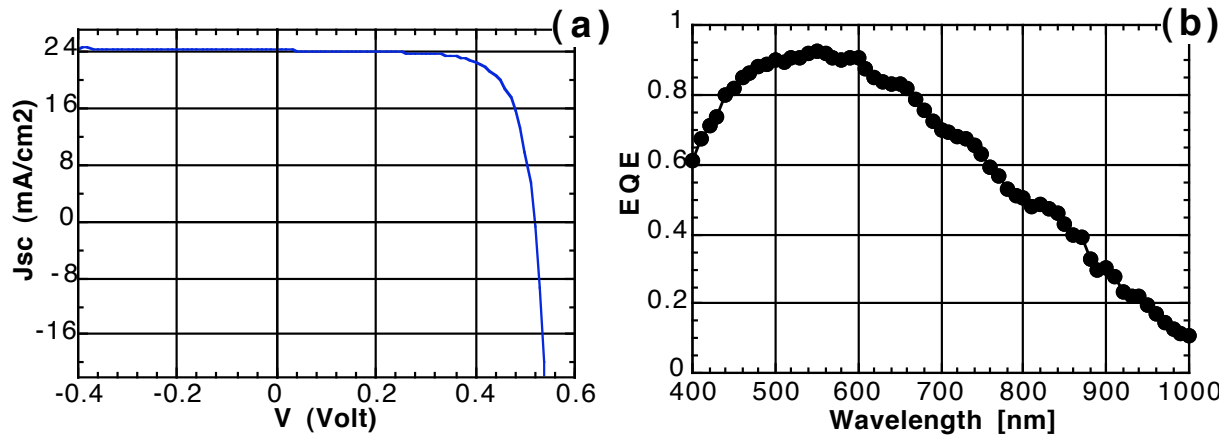


Figure 4: Our so far best \square c-Si:H solar cell in the n-i-p configuration deposited onto optimised light-scattering back-reflector of glass/silver/sputtered ZnO. AM1.5 conversion efficiency over 9%, V_{OC} =520 mV, FF=73%, J_{SC} =24.2 mA/cm², cell surface=0.3 cm², thickness=2.5 μ m.

For industrially relevant solar cell design, the introduction of highly scattering back-reflectors is necessary. These back-reflectors have to combine two constraints: a good optical performance as well as an optimally designed back-contact to the silicon layer.

The variation of silane concentration of the i-layer of the n-i-p cell is a rather old method (already known for the optimisation of amorphous solar cells [8]) but still applicable to solid \square c-Si:H solar cell fabrication process.

The remarkably good \square c-Si:H n-i-p solar cell (see figure 4) is the result of such an optimisation of the whole device at IMT Neuchâtel. A conversion efficiency exceeding 9% (V_{OC} =520 mV, FF=73%, J_{SC} =24.2 mA/cm²) shows exactly the combination of a good J_{SC} with a high V_{OC} . The only drawback of this cell is the low deposition rate of 2.6 Å/sec which is mainly due to the rather low VHF-plasma frequency of 70 MHz. Nevertheless, this is a promising result of a n-i-p solar cell approaching the region of 10% conversion efficiency.

ACKNOWLEDGEMENTS

This work was supported by the Swiss Federal Renewable Energy Program (grants 100 045 and 36 487) and the Swiss National Science Foundation (grant 66985.1).

REFERENCES

1. L. Feitknecht, O. Kluth, Y. Ziegler, X. Niquille, P. Torres, J. Meier, N. Wyrsh, A. Shah. Sol. En. Mat. & Solar Cells, Vol. 66, 2001, pp. 397-403.
2. J. Meier, S. Dubail, S. Golay, U. Kroll, S. Fay, E. Vallat-Sauvain, L. Feitknecht, J. Dubail, A. Shah, Sol. En. Mat. & Solar Cells, Vol. 74, 2002, pp. 457-467.
3. H. Fujiwara, M. Kondo, A. Matsuda, J. Appl. Phys., 93 (5): 2400-2409 MAR 1 2003
4. J. Bailat, E. Vallat-Sauvain, L. Feitknecht, C. Droz, A. Shah, ICAMS 2001, Nice, France, 2001, J. Non-Crystalline Solids Vol. 299-302, pp. 1219-1223.
5. P. Torres et al., Appl. Phys. Lett. 69 (10) 1996 p. 1373
6. J. Bailat, E. Vallat-Sauvain, L. Feitknecht, C. Droz and A. Shah. J. Appl. Phys., Vol. 93, No. 9, 1 May 2003
7. Y. Nasuno, M. Kondo and A. Matsuda, Jpn. J. Appl. Phys. Vol. 40 (2001) L303-L305, Part 2, No. 4A, 1 April 2001
8. R. Platz, S. Wagner, C. Hof, A. Shah et al., J. Appl. Phys. 84 (7): 3949-3953 OCT 1 1998